Available online at www.sciencedirect.com
ScienceDirect
International Journal of Pharmaceutics 357 (2008) 295–304
INTERNATIONAL JOURNAL OF PHARMACEUTICS
www.elsevier.com/locate/ijpharm

Pharmaceutical Nanotechnology

Lipid nanoparticles for prolonged topical delivery: An *in vitro* and *in vivo* investigation

Carmelo Puglia [a], Paolo Blasi [b,*], Luisa Rizza [a], Aurélie Schoubben [b], Francesco Bonina [a], Carlo Rossi [b], Maurizio Ricci [b]

[a] *Department of Pharmaceutical Sciences, School of Pharmacy, University of Catania, viale A. Doria 6, 95125 Catania, Italy*
[b] *Department of Chemistry and Technology of Drugs, School of Pharmacy, University of Perugia, via del Liceo 1, 06123 Perugia, Italy*

Received 13 October 2007; received in revised form 18 January 2008; accepted 25 January 2008
Available online 3 February 2008

Abstract

Dermal therapy is still a challenge due to the difficulties in controlling the active pharmaceutical ingredient (API) fate within the skin. Recently, lipid nanoparticles have shown a great potential as vehicle for topical administration of active substances, principally owing to the possible targeting effect and controlled release in different skin strata. Ketoprofen and naproxen loaded lipid nanoparticles were prepared, using hot high pressure homogenization and ultrasonication techniques, and characterized by means of photo correlation spectroscopy and differential scanning calorimetry. Nanoparticle behavior on human skin was assessed, *in vitro*, to determine drug percutaneous absorption (Franz cell method) and, *in vivo*, to establish the active localization (tape-stripping technique) and the controlled release abilities (UVB-induced erythema model). Results demonstrated that the particles were able to reduce drug penetration increasing, simultaneously, the permeation and the accumulation in the horny layer. A prolonged anti-inflammatory effect was observed in the case of drug loaded nanoparticles with respect to the drug solution. Direct as well as indirect evidences corroborate the early reports on the usefulness of lipid nanoparticles as carriers for topical administration, stimulating new and deeper investigations in the field.

Keywords: Ketoprofen; Naproxen; Lipid nanoparticles; SLN; NLC; Dermal targeting

1. Introduction

The treatment of skin diseases as well as of musculoskeletal disorders might benefit from topical administration, obtaining a substantial reduction of the systemic side effects and an improvement of the patient compliance. Drug topical administration is still a challenge in pharmaceutics and drug delivery due to the difficulties in controlling and, not less important, determining the exact amount of drug that reach the different skin layers (Schäfer-Korting et al., 2007). The API as well as the vehicle physicochemical characteristics are retained to be the main features responsible for the drug differential distribution in the skin (Beetge et al., 2000; Jacobi et al., 2006; Teichmann et al., 2007). The analytical issues are mostly due to technical and ethical reasons. In fact, blood or urine sampling are not useful since the data cannot be correlated with the amount of drug deposited in the skin while the direct analysis would require skin sampling with obvious problems of compliance and ethics (Wagner et al., 2002). Less invasive techniques, such as the SC stripping, by means of adhesive tape, and the quantification of the residual active in the applied formulation permit a non-complete but valuable evaluation (Wagner et al., 2002).

KET and NAP are two NSAIDs used for the treatment of musculoskeletal disorders (e.g., rheumatoid arthritis, osteoarthritis and ankylosing spondylitis) with non-optimal characteristics to be delivered through the skin (Swart et al., 2005). Different

Abbreviations: API, active pharmaceutical ingredient; DSC, differential scanning calorimetry; EI, erythema index; HPLC, high-performance liquid chromatography; HPH, hot high pressure homogenization; KET, ketoprofen; MED, minimal erythemal dose; NLC, nanostructured lipid carriers; NAP, naproxen; NSAIDs, non-steroidal anti-inflammatory drugs; PIE, percentage of inhibition of the erythema; P_m, permeability coefficient; PCS, photo correlation spectroscopy; RP, reverse phase; SLN, solid lipid nanoparticles; SCE, *stratum corneum epidermis*; SC, *stratum corneum*; US, ultrasonication.

* Corresponding author. Tel.: +39 0755855133; fax: +39 0755855163.
E-mail address: kaolino@unipg.it (P. Blasi).

0378-5173/$ – see front matter © 2008 Elsevier B.V. All rights reserved.
doi:10.1016/j.ijpharm.2008.01.045

strategies have been used to increase local soft tissue bioavailability of KET and NAP topically administered (Rautio et al., 1998; Bonina et al., 2001). Formulation of API within nanometric particulate carriers, in particular of lipid origin, has been used elsewhere with this aim (Maia et al., 2000; Mei et al., 2003). Lipid nanoparticles, due to the safety of the component materials and the controlled release abilities, possess a great potential and have generated a large interest in the industrial and academic worlds (Müller et al., 2002a; Müller, 2007). In fact, they have been proposed and investigated for many different applications and all the administration routes (Blasi et al., 2007; Chattopadhyay et al., 2007; Hauss, 2007; Müller et al., 2007; Schäfer-Korting et al., 2007).

In the scientific literature, a first generation of lipid nanoparticles can be found with the common name of SLN (Müller, 2007). Recently, SLN features have been considered advantageous for topical administration of active substances. The great potential of SLN to improve prednicarbate absorption through the skin was demonstrated (Maia et al., 2000). Another recent study reported that triptolide topical anti-inflammatory therapy was favored by its entrapment in SLN. This strategy guaranteed an improved availability of the drug at the site of action, reducing contemporary the needed dose and thus, dose dependent side effects like irritation and staining (Mei et al., 2003).

A second generation of lipid nanoparticles (Müller, 2007), known as NLC, have been recently developed and investigated for the same application. NLC are innovative vehicles introduced to overcome some limitations of SLN (Müller et al., 2002a; Hu et al., 2006). Particularly, NLC, composed of a solid lipid and a certain content of liquid lipid (oil), show an improved drug entrapment efficiency (Hu et al., 2005; Ricci et al., 2005) and an increased stability during storage with respect to SLN (Souto and Müller, 2006). When optimized, NLC exhibit high physical stability (Wissing and Müller, 2002), protection of loaded labile API against degradation (Jenning et al., 2000b), and excellent *in vivo* tolerability (Müller et al., 2002b). Furthermore, NLC, maintaining their solid state, can control the API release from the matrix (Müller et al., 2002b).

In a previous work regarding the evaluation of indomethacin percutaneous absorption from NLC, a decreased API permeation was observed and the formation of a drug reservoir in the SC, owing to the interaction between nanoparticles and SC lipids, was hypothesized (Ricci et al., 2005).

Even though the role of the vehicle in the API dermal or transdermal fate of topically administered formulations is known, this study may provide additional features to state if the abovementioned effect is general or just a particular case. This work may confirm the great potential of lipid nanoparticles as carriers for prolonged and targeted topical delivery.

To this aim, KET and NAP loaded NLC were prepared and characterized *in vitro* and *in vivo*. HPH and US methods were evaluated as possible preparation techniques, while PCS and DSC were employed for their characterization. Percutaneous absorption has also been studied, *in vitro*, using excised human skin membranes (i.e., SCE) and, *in vivo*, by determining the anti-inflammatory activity. Finally, in order to quantify the drug present in the SC, tape-stripping was performed.

2. Materials and methods

2.1. Materials

Compritol® 888 ATO (glyceryl behenate, tribehenin), a mixture of mono-, di- and triglycerides of behenic acid (C_{22}), was a gift of Gattefossé (Milan, Italy). Miglyol® 812 (caprylic/capric triglycerides) was provided by Eingemann & Veronelli S.p.A (Milan, Italy). Lutrol® F68 was a gift of BASF ChemTrade GmbH (Burgbernheim, Germany). Xanthan gum, KET and NAP were purchased from Sigma Aldrich corporation (St. Louis, MO, USA). Carbopol® 934P (CTFA: Carbomer) was obtained from BFGoodrich (Cleveland, Ohio, USA). HPLC grade acetonitrile and water were purchased from CarloErba reagents (CarloErba, Milan, Italy). When not specified, chemicals and reagents were of the highest purity grade commercially available.

2.2. NLC Preparation

2.2.1. Ultrasonication method

Blank and drug loaded NLC were prepared following the procedure reported elsewhere (Ricci et al., 2005). Briefly, Compritol® 888 ATO (4 g) was melted at 80 °C and Miglyol® 812 (1.52 g) and KET or NAP (80 mg) were added. The melted lipid phase was dispersed in the hot (80 °C) surfactant solution (Lutrol® F68, 1.35%, w/v) by using a high-speed stirrer (Ultra Turrax T25, IKA-Werke GmbH & Co. KG, Staufen, Germany) at 8000 rpm. The obtained pre-emulsion was ultrasonified by using a UP 400 S (Ultraschallprozessor, Dr. Hielscher GmbH, Germany) maintaining the temperature at least 5 °C above the lipid melting point. After US, the obtained dispersion was cooled in an ice bath in order to solidify the lipid matrix and to form NLC. Blank and drug loaded SLN were prepared and characterized as well.

2.2.2. Hot high pressure homogenization method

NLC were also prepared using the elsewhere reported HPH technique, slightly modified (Müller et al., 2002a). Briefly, the pre-emulsion was obtained following exactly the same procedure reported for the US method. The pre-emulsion was then homogenized using a homogenizer EmulsiFlex-C5 (Avestin, Ottawa, Canada) thermostated at 80 °C at a pressure of 100,000 kPa. Three homogenization cycles were performed. The hot dispersion was then cooled in an ice bath to obtain NLC.

2.2.3. Preparation of gel formulations

NLC were formulated into hydrogels using glycerol and xanthan gum as excipients (Ricci et al., 2005). Briefly, hydrogel formulations were produced adding to KET or NAP loaded NLC suspensions (89%, w/w) 10% (w/w) of glycerol and 1% (w/w) of xanthan gum. Control hydrogel formulations were prepared in the same way by using KET or NAP solutions (89%, w/w) instead of the NLC suspensions (Table 1). Hydrogels were stirred at 1000 rpm for 5 min and then stored at 4 °C before use.

Table 1
Composition (%, w/w) of KET (A and B) and NAP (C and D) formulations

Constituents	Formulation code			
	A	B[a]	C	D[b]
KET solution in distilled water	–	89	–	–
NAP solution in distilled water	–	–	–	89
KET loaded NLC suspension	89	–	–	–
NAP loaded NLC suspension	–	–	89	–
Glycerol	10	10	10	10
Xanthan gum	1	1	1	1

Hydrogels were stirred at 1000 rpm for 5 min and then stored at 4 °C before use.
[a] KET amount was correspondent to KET content in formulation A.
[b] NAP amount was correspondent to NAP content in formulation C.

2.3. Determination of KET and NAP loading

The percentage of KET and NAP entrapped in the lipid matrix was determined as follows: NLC dispersion was filtered by using a Pellicon XL tangential ultrafiltration system (Millipore, Milan, Italy) equipped with a polyethersulfone Biomax10 membrane. An amount of retained material was freeze-dried, dissolved in chloroform and analyzed by UV spectrophotometry at 257 and 270 nm for KET and NAP, respectively (Lambda 52, PerkinElmer, MA, USA). Calibration curves for the validated UV assays of KET and NAP, were performed on five solutions in the concentration ranges of 3–15 and 3–45 μg/ml, respectively. Correlation coefficient was >0.990. Each point represents the average of three measurements and the error was calculated as standard deviation (±S.D.). KET and NAP incorporation efficiency was expressed as drug content, calculated from Eq. (1).

$$\text{Drug content}\,(\%) = \frac{\text{Mass of drug in nanoparticles}}{\text{Mass of nanoparticles}} \times 100 \quad (1)$$

Possible lipid interferences during UV determination of KET and NAP were also investigated by comparing the two standard curves of each drug alone and in presence of lipids. The differences observed between the standard curves were within the experimental error, thus inferring that no lipid interference occurred (data not shown).

2.4. Particle size distribution

Mean particle size of the lipid dispersions was measured by PCS. A Zetamaster (Malvern Instrument Ltd., Sparing Lane South, Worcs, England), equipped with a solid state laser having a nominal power of 4.5 mW with a maximum output of 5 mW 670 nm, was employed. Analyses were performed using a 90° scattering angle at 20 ± 0.2 °C. Samples were prepared diluting 10 μl of NLC suspension with 2 ml of deionized water previously filtered through a 0.2 μm Acrodisc LC 13 PVDF filter (Pall-Gelman Laboratory, Ann Harbor, MI, USA). During the experiment, refractive index of the samples always matched liquid (toluene) to avoid stray light.

2.5. Differential scanning calorimetry

In order to characterize the thermal behavior of the lipid nanocarriers, DSC was performed using a heat flux instrument (DSC 2920, TA Instruments, USA) equipped with a refrigerated cooling system. A nitrogen purge at a flow rate of 60 cm^3/min was used to provide an inert gas atmosphere in the DSC cell. The system was calibrated using an indium standard and the sample was run against a hermetic empty reference pan. Prior to heating, the sample was equilibrated in the DSC pan (hermetic crimped aluminum pans) at 20 °C for 10 min. In all cases, a heating or cooling rate of 10 °C/min were used. Data were treated with Thermal Solutions software (TA Instruments, USA) and the results expressed as the mean of three determinations.

2.6. In vitro studies

2.6.1. Skin membrane preparation

Samples of adult human skin (mean age 36 ± 8 years) were obtained from breast reduction operations. Subcutaneous fat was carefully trimmed and the skin was immersed in distilled water at 60 ± 1 °C for 2 min (Kligman and Christophers, 1963), after which SCE were removed from the dermis using a dull scalpel blade. Epidermal membranes were dried in a desiccator at ∼25% relative humidity. The dried samples were wrapped in aluminium foil and stored at 4 ± 1 °C until use. Previous research works demonstrated the maintenance of SC barrier characteristics after storage in the reported conditions (Swarbrick et al., 1982). Besides, preliminary experiments were carried out in order to assess the barrier integrity of SCE samples by measuring the *in vitro* permeability of [^{3}H]water through the membranes using the Franz cell method described below. The value of calculated permeability coefficient (P_m) for [^{3}H]water agreed well with those previously reported (Bronaugh et al., 1986; Puglia et al., 2006).

2.6.2. In vitro skin permeation experiments

Samples of dried SCE were rehydrated by immersion in distilled water at room temperature for 1 h before being mounted in Franz-type diffusion cells supplied by LGA (Berkeley, CA). The exposed skin surface area was 0.75 cm^2 and the receiver compartment volume was of 4.5 ml.

The receptor compartment was filled with a water–ethanol solution (50:50) (to allow the establishment of the sink conditions and to sustain permeant solubilization) (Touitou and Fabin, 1988), stirred at 500 rpm and thermostated at 35 ± 1 °C during all the experiments.

Approximately 100 mg of each formulation (A–D) were placed on the skin surface in the donor compartment and the latter was covered with Parafilm®. Each experiment was run in duplicate for 24 h using three different donors. At predetermined intervals, samples (200 μl) of receiving solution were withdrawn and replaced with fresh solution. The samples were analyzed for drug content by HPLC as described below. KET and NAP fluxes through the skin were calculated by plotting the cumulative amounts of drug penetrating the skin against time and determining the slope of the linear portion of the curve and

the χ-intercept values (lag time) by linear regression analysis. Drug fluxes ($\mu g/cm^2\,h^{-1}$), at steady state, were calculated by dividing the slope of the linear portion of the curve by the area of the skin surface through which diffusion took place.

2.7. In vivo studies

2.7.1. Volunteers recruitment

In vivo experiments were performed on two groups of ten volunteers: group A enrolled for the first *in vivo* experimentation (evaluation of anti-inflammatory activity) and group B enrolled for the second one (tape-stripping). The volunteers were of both sexes in the age range 25–35 years and they were recruited after medical screening including the filling of a health questionnaire followed by physical examination of the application sites. After they were fully informed on the nature of the study and on the procedures involved, they gave their written consent. The participants did not suffer from any ailment and were not on any medication at the time of the study. They were rested for 15 min prior to the experiments and room conditions were set at $22 \pm 2\,^{\circ}C$ and 40–50% relative humidity.

2.7.2. In vivo anti-inflammatory activity

UVB-induced skin erythema was monitored by using a reflectance visible spectrophotometer X-Rite model 968 (X-Rite Inc. Grandville, MI, USA), calibrated and controlled as previously reported (Esposito et al., 2005; Ricci et al., 2005). Reflectance spectra were obtained over the wavelength range 400–700 nm using illuminant C and 2° standard observer. From the spectral data obtained, the erythema index (EI) was calculated using Eq. (2) (Dawson et al., 1980):

$$\mathrm{EI} = 100\left[\log\frac{1}{R_{560}} + 1.5\left(\log\frac{1}{R_{540}} + \log\frac{1}{R_{580}}\right) - 2\left(\log\frac{1}{R_{510}} + \log\frac{1}{R_{610}}\right)\right] \quad (2)$$

where $1/R$ is the inverse reflectance at a specific wavelength (560, 540, 580, 510 and 610).

The skin erythema was induced by UVB irradiation using a UVM-57 ultraviolet lamp (UVP, San Gabriel, CA, USA) whose specific parameters are reported elsewhere (Ricci et al., 2005). The MED was preliminarily determined, and an irradiation dose corresponding to twice the value of MED was used throughout the study.

For each subject (group A), seven sites on the ventral surface of each forearm were defined using a circular template ($1\,cm^2$) and demarcated with permanent ink. One of the seven sites of each forearm was used as control, three sites were treated with 100 mg of formulation A and the remaining three with 100 mg of formulation B. The preparations were spread uniformly by means of a solid glass rod and then the sites were occluded for 6 h using Hill Top Chambers (Hill Top Research, Cincinnati, OH). After the occlusion period, the chambers were removed and the skin surfaces were gently washed to remove the gel and allowed to dry for 15 min. Each pre-treated site was exposed to UV-B irradiation 1, 3 and 6 h ($t = 1$, $t = 3$ and $t = 6$, respectively) after gel removal and the induced erythema was monitored for 52 h. EI baseline values were taken at each designated site before application of gel formulation and they were subtracted from the EI values obtained after UV-B irradiation at each time point to obtain ΔEI values. For each site, the AUC was computed using the trapezoidal rule.

The volunteers were again recruited to complete the experimentation after a wash-out period of two weeks and the same experimental procedure was repeated for the formulations C and D.

To better outline the results obtained, the PIE was calculated from the AUC values using Eq. (3):

$$\mathrm{PIE} = \frac{\mathrm{AUC_{(C)}} - \mathrm{AUC_{(T)}}}{\mathrm{AUC_{(C)}}} \times 100 \quad (3)$$

where $AUC_{(C)}$ is the area under the response/time curve of the vehicle-treated site (control) and $AUC_{(T)}$ is the area under the response/time curve of the drug-treated site.

2.7.3. Tape-stripping

The first steps of the experimental protocol previously described were employed in this second *in vivo* study (Ricci et al., 2005). For each subject of group B, six sites ($2\,cm^2$) on the ventral surface of each forearm were defined and 200 mg of formulations A and B were applied uniformly on the site by means of a solid glass rod and were then occluded for 6 h. After the occlusion period, the residual formulations were removed by gently wiping with cotton balls (different for each pre-treated site). Twenty individual $2\,cm^2$ squares of adhesive tape (Scotch® Book Tape 845, 3M) were utilized to sequentially tape-strip the SC from the application sites. To obtain a realistic comparison between the experiments, the removal of SC in each pre-treated site was effected at 1, 3 and 6 h ($t = 1$, $t = 3$ and $t = 6$, respectively) after gel removal.

Since this experimental procedure had required the total surface of their forearms, the volunteers were recruited again, after a wash-out period of two weeks, to complete the *in vivo* experimentation. Again, for each subject, six sites ($2\,cm^2$) on the ventral surface of each forearm were treated with 200 mg of formulations C and D and, after that, the same protocol, previously described, was performed.

In order to quantify the amount of drug contained in the SC, adhesive squares were weighed on a Sartorius balance (model ME415S, sensitivity 1 μg), before and after tape-stripping, to quantify the weight of SC removed. API were extracted from the tape (acetonitrile, 16 h) and KET and NAP contents were determined by HPLC. The recovery of KET and NAP was validated by spiking tape-stripped samples of untreated SC with 100 μl of a 10mg/ml solution of drug in acetonitrile (~1 mg/tape of drug). The extraction efficiency was $90.9 \pm 0.7\%$ for KET ($n = 3$) and $94.3 \pm 0.2\%$ for NAP ($n = 3$).

2.8. High-performance liquid chromatography

The HPLC apparatus consisted of a Shimadzu LC10 AT Vp (Milan, Italy) equipped with a 20 μl loop injector and

Table 2
Particle size and drug loading of SLN and NLC containing KET and NAP

Batch	Sample	Preparation method	Mean particle size ± S.D. (nm)	Drug content (%)
1	KET loaded NLC	US	335.1 ± 12.9	1.12
2	KET loaded NLC	HPH	215.7 ± 89.9	0.66
3	NAP loaded NLC	US	380.0 ± 13.6	1.25
4	NAP loaded NLC	HPH	404.2 ± 49.9	1.39

a SPD-M 10 A Vp Shimadzu photodiode array UV detector.

Chromatography was performed using a Jupiter Phenomenex C_{18} RP column (particle size, 5 μm; 250 × 4.6 mm i.d.; Phenomenex, Torrance, CA, USA). The mobile phase was composed of 30% water (pH 3 adjusted with phosphoric acid) and 70% acetonitrile and the detection was effected at 257 and 270 nm for KET and NAP, respectively. The flow rate was set at 1 ml/min. The retention time was 4.1 min and 3.2 min for KET and NAP, respectively.

2.9. Statistical analysis

Statistical analysis of *in vitro* data was performed using the Student's *t*-test. Statistical differences of *in vivo* data were determined using repeated measure analysis of variance (ANOVA) followed by the Bonferroni-Dunn post hoc pair-wise comparison procedure. A probability, *P*, of less than 0.05 was considered significant in this study.

3. Results and discussion

3.1. NLC preparation and characterization

KET and NAP loaded NLC were successfully prepared with about 30% of oil within the solid lipid matrix. The inclusion of oils, such as Miglyol®, α-tocopherol or others (Souto and Müller, 2006), is useful both in NLC formulation optimization (Müller et al., 2002a) and in enhancing the dermal/transdermal delivery (Müller et al., 2002b). The oil, because of its liquid state, may also hold higher amounts of drugs and, behaving as an impurity in the solid lipid, reduces the particle crystallinity conferring better stability and higher suitability for the controlled release (Müller et al., 2002a,b).

The structure of these particles, i.e., the presence or not of nanocompartments or nanostructures within the matrix, is still matter of debate (Müller et al., 2002a; Jores et al., 2003, 2005; Castelli et al., 2005). It should be kept in mind that the chemical nature, purity, and concentration of every ingredient (e.g., lipid, surfactant, and active), in addition to the preparation procedure, will strongly influence the structure of NLC. Afterward, most unlikely it will be possible to have a general statement on this topic and considerations on the single case would be more suitable (Schäfer-Korting et al., 2007).

In this specific case, the use of Miglyol® was useful to increase the drug loading with respect to SLN. These findings can be ascribed to the higher solubility of KET and NAP in Miglyol® compared to the drug solubility within the sole Compritol®. Furthermore, Miglyol® addition tends to promote the formation of a small particle population as result of a higher molecular mobility of the matrix.

Table 2 shows the particle size and drug loading of the prepared batches. Both preparation methods were suitable for the production of lipid particles in the nanometer scale range. These two procedures are very versatile and have the advantage to avoid the use of organic solvents, leading to potential toxic contaminations. Metallic particle contamination, that can occur with probe sonication, may be avoided adopting appropriate instrumentation. Besides, HPH is generally the most suitable procedure because of its easy scalability. In this specific case, HPH produced similar or even smaller particles compared to US but, according to the drug content values, the latest appeared more appropriate. For these reasons, the batches 1 and 3 (Table 2) were chosen for further *in vitro* and *in vivo* investigations.

Table 3 and Fig. 1 show the DSC data of the different batches. Blank and drug loaded SLN were also prepared and characterized for comparison. Bulk Compritol® showed a sharp endothermic event, ascribing to the melting, around 72 °C (minimum) with an extrapolated onset of the melting peak ~69 °C (the difference between onset and minimum can be taken as a measure for the width of the peak). When the raw material was formulated as nanoparticles, the endothermic peak was broader and happened at a slightly lower temperature (Table 3). These differences are generally ascribed to the nanometric size of the particles, having then a high specific surface area (Westesen and Bunjes, 1995; Bunjes et al., 2000). A certain effect due to the surfactant should be taken into account as well (Jenning et al., 2000c). The addition of oil (i.e., Miglyol®) into the matrix provoked an additional shift of the melting point to lower temperatures, with the difference between the onset and the minimum of the peak of about 10 °C (Table 3). The loading of the drugs, namely KET and NAP, did not provoke any considerable effect in the lipid matrix thermal behavior under these experimental conditions.

Table 3
DSC data of the different lipid nanoparticle preparations

Sample	Onset (°C)	Melting point (°C)
Compritol®	69.69 ± 0.09	72.26 ± 0.28
Blank SLN	67.24 ± 0.38	71.78 ± 0.12
Blank NLC	58.93 ± 0.72	68.49 ± 0.12
KET loaded SLN	67.61 ± 0.04	71.72 ± 0.01
NAP loaded SLN	67.60 ± 0.04	71.89 ± 0.04
KET loaded NLC	61.23 ± 0.28	68.81 ± 0.09
NAP loaded NLC	60.76 ± 0.62	68.67 ± 0.33

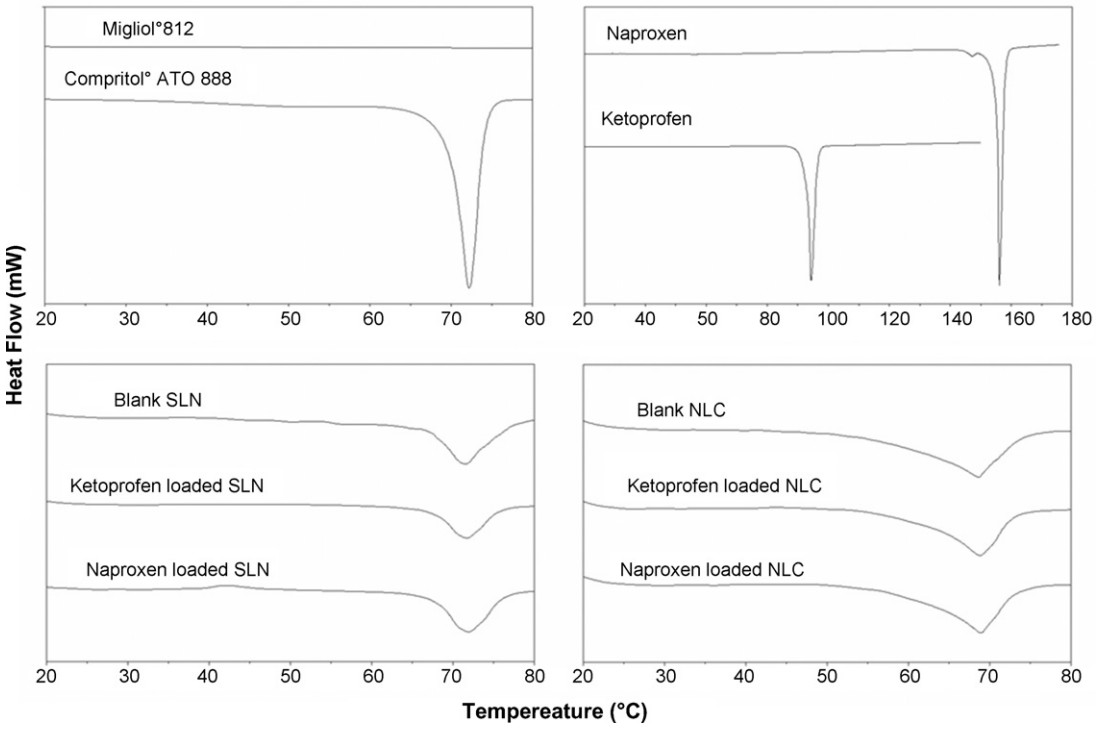

Fig. 1. DSC data of the raw lipid materials (i.e., Compritol® 888 ATO and Miglyol® 812), crystalline API (i.e., KET and NAP), as well as blank and drug loaded SLN and NLC. Exothermic up.

3.2. *In vitro skin permeation experiments*

Fig. 2 shows the cumulative plots of the amount of KET and NAP permeated through human SCE membranes as a function of time. Drug flux values for formulations A–D are reported in Fig. 3. Statistical analysis revealed a significant difference ($P < 0.01$) between the steady-state flux values obtained for A and C. Moreover both A and C showed flux values considerably lower than B and D ($P < 0.01$), respectively.

As expected, KET and NAP formulated in NLC showed a decreased permeation through the skin that can be explained hypothesizing a drug accumulation in the horny layer. In fact, either lipidic or polymeric nanoparticles have shown the peculiarity to reduce and/or suppress the permeation (transdermal delivery) through the skin while enhancing the penetration (dermal delivery) into the upper skin layers (Jenning et al., 2000a; de Jalón et al., 2001; Alvarez-Román et al., 2004; Lombardi Borgia et al., 2005; Chen et al., 2006; Liu et al., 2007). The obtained results confirm the key role of the vehicle in determining the API dermal or transdermal fate for topically applied formulations.

The differences observed between A and C may be ascribed to the different drug physicochemical characteristics (e.g., pK_a, solubility, log P) originating diverse interactions with the nanoparticle and/or SC lipids (Beetge et al., 2000; Schäfer-Korting et al., 2007). Indeed, a similar difference was also seen for the gels containing the free drugs. In particular, log P (KET

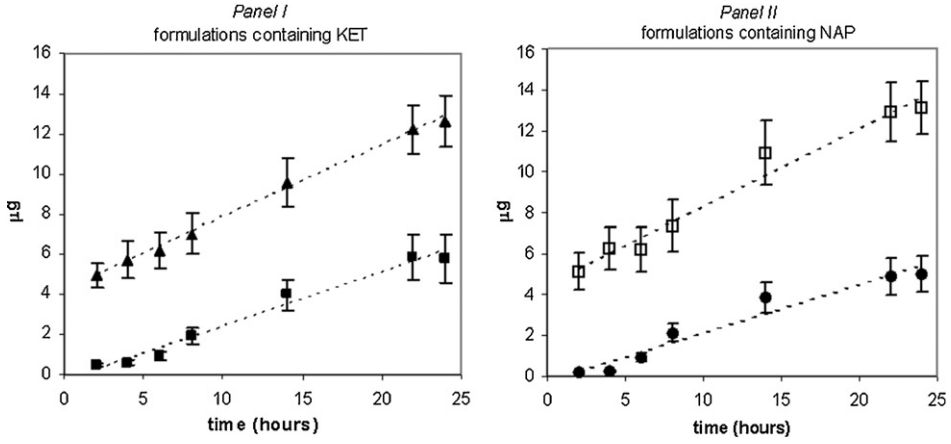

Fig. 2. Permeation profiles of KET (panel I) and NAP (panel II) from different formulations through SCE membranes using Franz-type diffusion cells. ■, Formulation A containing KET loaded NLC; ▲, formulation B containing free KET; ●, formulation C containing NAP loaded NLC; □, formulation D containing free NAP.

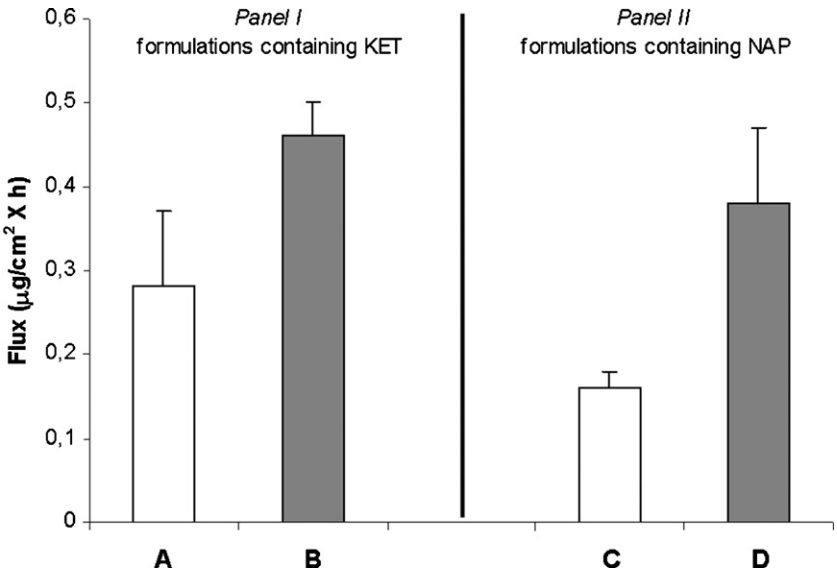

Fig. 3. Steady-state fluxes of KET (panel I) and NAP (panel II) through excised human skin from A–D formulations.

log *P*, 0.97; NAP log *P*, 3.22), exhibiting a larger difference than pK_a values (KET pK_a, 4.45; NAP pK_a, 4.20), seems to be the main parameter responsible for this behavior (Beetge et al., 2000). It is estimated that a therapeutic molecule should posses a log *P* equal or smaller than 2 to be a potential candidate for transdermal delivery. NAP, having higher log *P* value, tends to accumulate in the SC and, afterward, to be less available in the receptor compartment.

It is argued that this feature could be responsible for drug accumulation to the upper skin layer explaining, at least in part, the lower penetration observed with the formulation C (Lombardi Borgia et al., 2005). This hypothesis agrees well with the results obtained for the tape-stripping experiments and the *in vivo* anti-inflammatory activity reported below.

3.3. Tape-stripping

Approximately, the same amount of SC was removed by each tape-stripping experiment. As previously reported, the SC amount was higher in the initial ten strips while, gradually, reached a constant amount for the latter strippings (data not shown) (Jacobi et al., 2005). The amounts of drug recovered in the SC at each time point for NLC based formulations (A and C) were significantly higher than those recovered from the corresponding formulations containing the free drugs ($P < 0.05$) (Fig. 4). It can be hypothesized that the detected amounts of drugs were stored in the upper half of the SC. In fact, the first 20 tape-strips have been shown to correspond to about 66% of the SC (Jacobi et al., 2005).

After 6 h, neither KET or NAP were detectable in the horny layer of the skin treated with the gels containing the free drugs while, still ~about 10 μg/cm^2 were measurable in the case of NLC containing gels (Fig. 4). These findings confirm the previous assumption that NLC provoke the accumulation of the embedded API into the upper skin layers, reducing thus the drug flux and creating a reservoir able to prolong the skin residence time. The epidermal reservoir was first hypothesized by Malkinson and Ferguson (1955) for hydrocortisone and

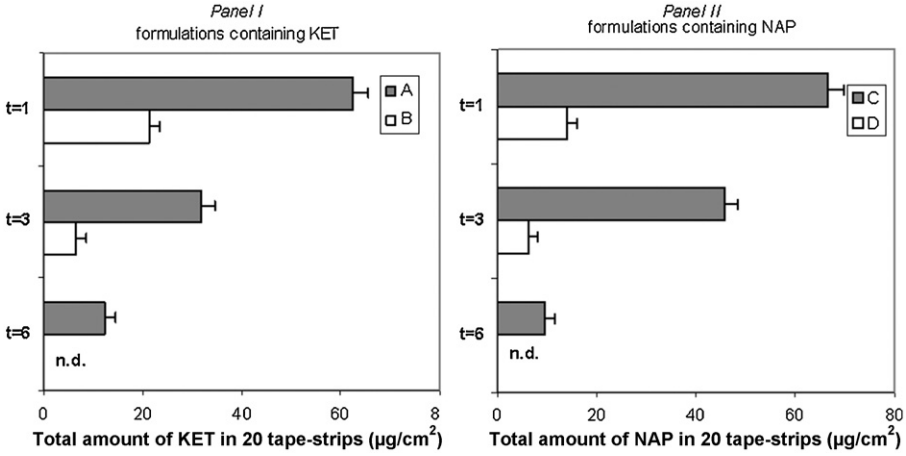

Fig. 4. Total amount of KET (panel I) and NAP (panel II) within the tape-stripped *stratum corneum* after 1, 3 and 6 h from the removal of A–D formulations. Data represent the mean for ten subjects. n.d. (not detectable).

was later confirmed by other evidences (Hadgraft, 1979). In the specific case of corticosteroids, two main characteristics were accounted as possible accumulation mechanisms, i.e., the vasoconstriction and the lipophilic character (SC/water partition coefficient). Even if vasoconstriction is generally absent in NSAIDs, a short-term reservoir may be considered possible due to the drug/vehicle physicochemical properties.

Similar results have been previously reported (Jenning et al., 2000a; de Jalón et al., 2001; Alvarez-Román et al., 2004; Lombardi Borgia et al., 2005; Chen et al., 2006; Liu et al., 2007). For instance, vitamin A penetrated more efficiently the horny layer when applied as SLN formulation with respect to nanoemulsion (Jenning et al., 2000a). Isotretinoin loaded SLN were found to increase the amount of drug in the skin when compared to the control tincture; additionally, the active did not reach the receptor chamber in detectable amounts as it was seen for the tincture (Liu et al., 2007). Analogous results were reported for prednicarbate and coenzyme Q10 loaded SLN when compared to conventional formulations (Maia et al., 2002; Müller et al., 2002b).

The mechanism by which this happens is not clear and different hypothesis have to be accounted. In general, intact particles are not considered to permeate the horny layer and, due to the rigid nature of NLC, drug penetration mechanism should be similar to that of drugs within gel-state liposomes (Bouwstra et al., 2003; Schäfer-Korting et al., 2007). The follicular pathway, generally neglected due to the low number of follicles present in the human skin (i.e., ~0.1% of the skin surface), may be more considerable in the case of particulate drugs or carriers (3–10 μm in size) but this should not be the case because of the small particle size. The contribution of the lipophilicity on follicular drug absorption is a complex subject in and of itself and cannot be addressed with this experimental setup (Ogiso et al., 1996; Frum et al., 2007). The effects due to water loss (e.g., crystal modification, drug expulsion and/or concentration) can be also ignored because the formulations were applied with occlusion.

On the contrary, the lipid bioadhesive properties have to be accounted as they may play a relevant role. It can be speculated that NLC adhesion to the horny layer might be, at least in part, responsible for the observed effect. However, it cannot be excluded that the tight adhesion made less efficacious the formulation washing and a certain amount of NLC was not removed and its content quantified.

At this point, a reflection on the similarities between the composition of NLC and the skin is also needed. The SC is mainly composed by three classes of lipids, i.e., ceramides, free fatty acids and cholesterol. The most abundant acyl chain lengths are C24–C26 in ceramides and C22–C24 in free fatty acids (Bouwstra et al., 2003). Compritol® 888 ATO is a mixture of mono-, di- and triglycerides (monoglycerides, 15–23%; diglycerides, 40–60%; triglycerides, 21–35%) of behenic acid (C22) (behenic acid content >83%) (COMPRITOL® 888 ATO Data Sheet). These analogies (i.e., C22) might reasonably play a role on the NLC/SC interaction and, consequently, on the adhesion and reservoir formation. Moreover, the presence of other fatty acids (COMPRITOL® 888 ATO Data Sheet), together with the presence of Miglyol®, may enhance the capacity of NLC components to mix with the SC and to retard the active permeation on deeper skin strata (Bouwstra et al., 2003). Since drug localization in the particles seems also to play a significant role in skin targeting, this feature should be accounted as well. For example, drug targeting was achieved when betamethasone valerate, due to its physicochemical characteristics, accumulate on the particle surface. On the contrary, no targeting was achieved with the glucocorticoid monoester homogenously distributed within the matrix (Sivaramakrishnan et al., 2004). This effect seems to be related to the burst release due to drug superficial location.

3.4. In vivo anti-inflammatory activity

KET and NAP delivery into the skin following topical application of A–D formulations was indirectly evaluated *in vivo* by monitoring the effect on UVB-induced erythema. Skin reflectance spectrophotometry was used to determine the extent of the erythema and to assess the A–D inhibition capacity after their preventive application onto the skin. The AUC was determined for each subject plotting ΔEI values versus time. An inverse relationship was found between the AUC and the inhibi-

Table 4
$AUC_{0–52}$ values obtained pre-treating skin sites with different topical formulations containing KET (A–B) or NAP (C–D) and applying UVB radiations after 1 h ($t = 1$), 3 h ($t = 3$) or 6 h ($t = 6$) from their removal

Subjects	$AUC_{0–52}$												
	$t = 1$				$t = 3$				$t = 6$				Control
	Form A	Form B	Form C	Form D	Form A	Form B	Form C	Form D	Form A	Form B	Form C	Form D	
A	944.8	585.3	887.6	499.4	634.9	941.6	763.4	928.8	610.2	1034.2	617.2	1118.6	1158.6
B	857.4	498.4	890.1	497.3	596.6	1121.3	816.2	891.3	598.4	1286.3	590.1	979.3	1326.2
C	790.8	611.2	918.4	578.9	711.3	898.4	762.1	794.5	863.3	1021.4	641.4	998.3	1215.6
D	1011.3	590.3	802.3	563.4	700.1	925.6	781.3	834.4	641.6	946.2	599.3	935.6	1018.2
E	926.4	583.4	898.7	642.2	629.6	1148.3	707.4	961.1	597.2	1018.7	631.1	1067.4	1012.3
F	828.3	726.6	1087.4	509.4	594.4	1022.1	881.6	795.6	600.4	1115.9	622.4	1082.1	984.4
G	893.2	599.2	872.4	555.1	644.4	1009.5	689.3	950.9	651.7	1070.4	618.5	1035.1	1119.2
H	798.6	602.4	826.3	561.6	627.9	1107.3	740.5	978.2	623.1	994.3	606.3	986.8	1217.1
I	803.1	594.6	1019.8	520.4	606.3	1024.1	850.3	939.4	616.6	965.8	600.1	1025.3	1029.3
L	908.2	623.3	1048.6	496.3	708.4	987.9	787.3	848.8	684.6	1009.9	617.6	917.6	1218.0
Mean	876.2	601.5	925.1	542.4	645.4	1018.6	777.9	892.3	648.7	1046.3	614.4	1014.6	1129.9

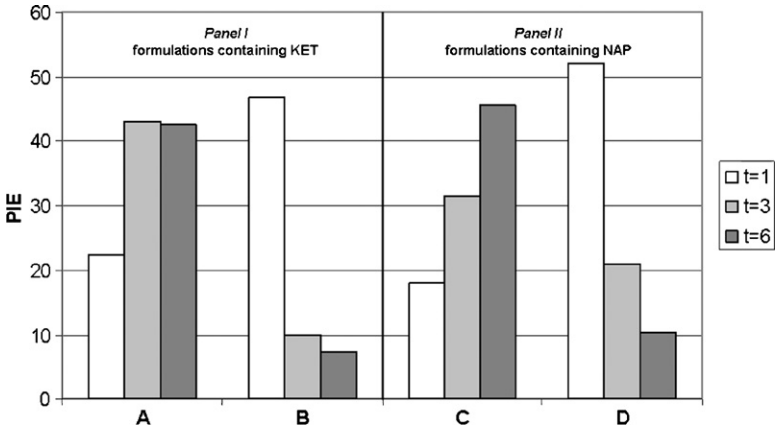

Fig. 5. Percentage of inhibition of the erythema by the different topical formulations containing KET (A and B) or NAP (C and D). Data represent the mean for ten subjects.

tion of UVB-induced erythema (Table 4). Fig. 5 reports the PIE values.

Formulations B and D showed to be more effective than A and C in inhibiting the induced erythema 1 h after gel removal ($P < 0.05$), while at 3 and 6 h the situation was reversed (Table 4 and Fig. 5). The higher drug fluxes registered for the gels containing the free drugs may plausibly explain this behavior. Since UVB radiation penetrates only the upper layers of the epidermis, NSAID concentrations in the strata underling the SC will matter for the anti-inflammatory activity (Matsumura and Ananthaswamy, 2004; Young, 2006). The higher drug fluxes might be responsible for a quicker achievement of NSAID therapeutic concentrations within the interested skin layers and for the fast disappearance of the effect.

Formulation A and C showed a different behavior (Fig. 5). Formulation A reached a PIE of about 40% after 3 h that was maintained for additional 3 h, although C gradually increased from ∼20% ($t = 1$) to ∼45% within the 5 remaining hours (Fig. 5). The same but opposite trend was observed in the decrease of the PIE for the gel containing the free drugs. Even though the explanation of this behavior will not be easy due to the indirect evidence, an attempt of elucidation was made. Since this behavior was observed with and without the lipid carrier, it might be reasonably ascribed to the diverse physicochemical, pharmacokinetic, and pharmacodynamic properties of KET and NAP. For instance, log P (KET log P, 0.97; NAP log P, 3.22), that was seen to influence both the drug residence time in the depot (eventually formed in the SC) and the skin penetration, may generate these differences (Hadgraft, 1979; Beetge et al., 2000). Besides, diverse pharmacokinetic characteristics, together with a dissimilar anti-inflammatory activity (in part linked to a more complex mechanism of action than the sole inhibition of cyclooxygenases) (Bizzarri et al., 2001; Kladana et al., 2006), have to be accounted as well.

4. Conclusions

The obtained results confirmed the potential of NLC as carriers for topical administration demonstrating drug penetration reduction and, at the same time, its accumulation in the horny layer. Even though, the mechanisms by which this phenomenon occurs are not completely understood, the particles were able to extend the anti-inflammatory effect of the embedded active molecules providing their prolonged release in the epidermis. This study provides supplementary evidences that NLC have a targeting and prolonged release effect with great potentials in dermal delivery.

References

Alvarez-Román, R., Naik, A., Kalia, Y.N., Guy, R.H., Fessi, H., 2004. Enhancement of topical delivery from biodegradable nanoparticles. Pharm. Res. 21, 1818–1825.

Beetge, E., du Plessis, J., Müller, D.G., Goosen, C., van Rensburg, F.J., 2000. The influence of the physicochemical characteristics and pharmacokinetic properties of selected NSAID's on their transdermal absorption. Int. J. Pharm. 193, 261–264.

Bizzarri, C., Pagliei, S., Brandolini, L., Ma scagni, P., Caselli, G., Transidico, P., Sozzoni, S., Bestini, R., 2001. Selective inhibition of interleukin-8-induced neutrophil chemotaxis by ketoprofen isomers. Biochem. Pharmacol. 61, 1429–1437.

Blasi, P., Giovagnoli, S., Schoubben, A., Ricci, M., Rossi, C., 2007. Solid lipid nanoparticles for targeted brain drug delivery. Adv. Drug Deliv. Rev. 59, 454–477.

Bonina, F.P., Puglia, C., Barbuzzi, T., de Caprariis, P., Palagiano, F., Rimoli, M.G., Saija, A., 2001. In vitro and in vivo evaluation of polyoxyethylene esters as dermal prodrugs of ketoprofen, naproxen and diclofenac. Eur. J. Pharm. Sci. 14, 123–134.

Bouwstra, J.A., Honeywell-Nguyen, P.L., Gooris, G.S., Ponec, M., 2003. Structure of the skin barrier and its modulation by vesicular formulations. Prog. Lipid Res. 42, 1–36.

Bronaugh, R.L., Stewart, R.F., Simon, M., 1986. Methods for in vitro percutaneous absorption studies VII: use of excised human skin. J. Pharm. Sci. 75, 1094–1097.

Bunjes, H., Koch, M.H.J., Westesen, K., 2000. Effect of particle size on colloidal solid triglycerides. Langmuir 16, 5234–5241.

Castelli, F., Puglia, C., Sarpietro, M.G., Rizza, L., Bonina, F., 2005. Characterization of indomethacin loaded lipid nanoparticles by differential scanning calorimetry. Int. J. Pharm. 304, 231–238.

Chattopadhyay, P., Shekunov, B.Y., Yim, D., Cipolla, D., Boyd, B., Farr, S., 2007. Production of solid lipid nanoparticles suspensions using supercritical fluid extraction of emulsions (SFEE) for pulmonary delivery using the AERx system. Adv. Drug Deliv. Rev. 59, 444–453.

Chen, H., Chang, X., Du, D., Liu, W., Liu, J., Weng, T., Yang, Y., Xu, H., Yang, X., 2006. Podophyllotoxin-loaded solid lipid nanoparticles for epidermal targeting. J. Control. Release 110, 296–306.

COMPRITOL® 888 ATO Data Sheet, Gattefossé, specification number 3123/06, last update 22/04/05.

Dawson, J.B., Barker, D.J., Ellis, D.J., Grassam, E., Catterill, J.A., Fischer, G.W., Feather, J.W., 1980. A theoretical and experimental study of light absorption and scattering by in vivo skin. Phys. Med. Biol. 25, 696–709.

de Jalón, E.G., Blanco-Príeto, M.J., Ygartua, P., Santoyo, S., 2001. Topical application of acyclovir-loaded microparticles: quantification of the drug in porcine skin layers. J. Control. Release 75, 191–197.

Esposito, E., Cortesi, R., Drechsler, M., Paccamiccio, L., Mariani, P., Contado, C., Stellin, E., Menegatti, E., Bonina, F., Puglia, C., 2005. Cubosome dispersions as delivery systems for percutaneous administration of indomethacin. Pharm. Res. 22, 2163–2173.

Frum, Y., Bonner, M.C., Eccleston, G.M., Meidan, V.M., 2007. The influence of drug partition coefficient on follicular penetration: in vitro human skin studies. Eur. J. Pharm. Sci. 30, 280–287.

Hadgraft, J., 1979. The epidermal reservoir: a theoretical approach. Int. J. Pharm. 2, 265–274.

Hauss, D.J., 2007. Oral lipid-based formulations. Adv. Drug. Deliv. Rev. 59, 667–676.

Hu, F.Q., Jiang, S.P., Du, Y.Z., 2005. Preparation and characterization of stearic acid nanostructured lipid carriers by solvent diffusion method in an aqueous system. Colloid Surf. B 45, 167–173.

Hu, F.Q., Jiang, S.P., Du, Y.Z., Yuan, H., Ye, Y., Zeng, S., 2006. Preparation and characteristics of monostearin nanostructured lipid carriers. Int. J. Pharm. 314, 83–89.

Jacobi, U., Tassopoulos, T., Surber, C., Lademann, J., 2006. Cutaneous distribution and localization of dyes affected by vehicles all with different lipophilicity. Arch. Dermatol. Res. 297, 303–310.

Jacobi, U., Weigmann, H.J., Ulrich, J., Sterry, W., Lademann, J., 2005. Estimation of the relative stratum corneum amount removed by tape stripping. Skin Res. Technol. 11, 91–96.

Jenning, V., Gysler, A., Schäfer-Korting, M., Gohla, S.H., 2000a. Vitamin A loaded solid lipid nanoparticles for topical use: occlusive properties and drug targeting to the upper skin. Eur. J. Pharm. Biopharm. 49, 211–218.

Jenning, V., Schafer-Korting, M., Ghola, S., 2000b. Vitamin A-loaded solid lipid nanoparticles for topical use: drug release properties. J. Control. Release 66, 115–126.

Jenning, V., Thünemann, A.F., Gohla, S.H., 2000c. Characterisation of a novel solid lipid nanoparticle carrier system based on binary mixtures of liquid and solid lipids. Int. J. Pharm. 199, 167–177.

Jores, K., Mehnert, W., Mäder, K., 2003. Physicochemical investigations on solid lipid nanoparticles and on oil-loaded solid lipid nanoparticles: a nuclear magnetic resonance and electron spin resonance study. Pharm. Res. 20, 1274–1283.

Jores, K., Haberland, A., Wartewig, S., Mäder, K., Mehnert, W., 2005. Solid lipid nanoparticles (SLN) and oil-loaded SLN studied by spectrofluorometry and raman spectroscopy. Pharm. Res. 22, 1887–1897.

Kladana, A., Aboul-Enein, H.Y., Kruk, I., Lichszteld, K., Michalska, T., 2006. Scavenging of reactive oxygen species by some nonsteroidal anti-inflammatory drugs and fenofibrate. Biopolymers 82, 99–105.

Kligman, A.M., Christophers, E., 1963. Preparation of isolated sheets of human stratum corneum. Arch. Dermatol. 88, 702–705.

Liu, J., Hu, W., Chen, H., Ni, Q., Xu, H., Yang, X., 2007. Isotretinoin-loaded solid lipid nanoparticles with skin targeting for topical delivery. Int. J. Pharm. 328, 191–195.

Lombardi Borgia, S., Regehly, M., Sivaramakrishnan, R., Mehnert, W., Korting, H.C., Danker, K., Röder, B., Kramer, K.D., Schäfer-Korting, M., 2005. Lipid nanoparticles for skin penetration enhancement-correlation to drug localization within the particle matrix as determined by fluorescence and parelectric spectroscopy. J. Control. Release 110, 151–163.

Maia, C.S., Mehnert, W., Schäfer-Korting, M., 2000. Solid lipid nanoparticles as drug carriers for topical glucocorticoids. Int. J. Pharm. 196, 165–167.

Maia, C.S., Mehnert, W., Schaller, M., Korting, H.C., Gysler, A., Haberland, A., Schäfer-Korting, M., 2002. Drug targeting by solid lipid nanoparticles for dermal use. J. Drug Target. 10, 489–495.

Malkinson, F.D., Ferguson, E.H., 1955. Percutaneous absorption of hydrocortisone-4-C14 in two human subjects. J. Invest. Dermatol. 25, 281–283.

Matsumura, Y., Ananthaswamy, H.N., 2004. Toxic effects of ultraviolet radiation on the skin. Toxicol. Appl. Pharmacol. 195, 298–308.

Mei, Z., Chen, H., Weng, T., Yang, Y., Yang, X., 2003. Solid lipid nanoparticle and microemulsion for topical delivery of triptolide. Eur. J. Pharm. Biopharm. 56, 189–196.

Müller, R.H., Radtke, M., Wissing, S.A., 2002a. Nanostructured lipid matrices for improved microencapsulation of drugs. Int. J. Pharm. 242, 121–128.

Müller, R.H., Radtke, M., Wissing, S.A., 2002b. Solid lipid nanoparticles (SLN) and nanostructured lipid carriers (NLC) in cosmetic and dermatological preparations. Adv. Drug Deliv. Rev. 54, S131–S155.

Müller, R.H., 2007. Lipid nanoparticles: recent advances. Adv. Drug Deliv. Rev. 59, 375–376.

Müller, R.H., Petersen, R.D., Hommoss, A., Pardeike, J., 2007. Nanostructured lipid carriers (NLC) in cosmetic dermal products. Adv. Drug Deliv. Rev. 59, 522–530.

Ogiso, T., Niinaka, N., Iwaki, M., 1996. Mechanism for enhancement effect of lipid disperse system on percutaneous absorption. J. Pharm. Sci. 85, 57–64.

Puglia, C., Filosa, R., Peduto, A., de Caprariis, P., Rizza, L., Bonina, F., Blasi, P., 2006. Evaluation of alternative strategies to optimize ketorolac transdermal delivery. AAPS PharmSciTech 7, article 64 E1–E9.

Rautio, J., Taipale, H., Gynther, J., Vepsaelaeinen, J., Nevalainen, T., Jaervinen, T., 1998. In vitro evaluation of acyloxyalkyl esters as dermal prodrugs of ketoprofen and naproxen. J. Pharm. Sci. 87, 1622–1628.

Ricci, M., Puglia, C., Bonina, F., Di Giovanni, C., Giovagnoli, S., Rossi, C., 2005. Evaluation of indomethacin percutaneous absorption from nanostructured lipid carriers (NLC): *in vitro* and in vivo studies. J. Pharm. Sci. 94, 1149–1159.

Schäfer-Korting, M., Mehnert, W., Korting, H.C., 2007. Lipid nanoparticles for improved topical application of drugs for skin diseases. Adv. Drug Deliv. Rev. 59, 427–443.

Sivaramakrishnan, R., Nakamura, C., Mehnert, W., Korting, H.C., Kramer, K.D., Schäfer-Korting, M., 2004. Glucocorticoid entrapment into lipid carriers-characterisation by parelectric spectroscopy and influence on dermal uptake. J. Control. Release 97, 493–502.

Souto, E.B., Müller, R.H., 2006. Investigation of the factors influencing the incorporation of clotrimazole in SLN and NLC prepared by hot high-pressure homogenization. J. Microencapsul. 23, 377–388.

Swarbrick, J., Lee, G., Brom, J., 1982. Drug permeation through human skin. I. Effects of storage conditions of skin. J. Invest. Dermatol. 78, 63–66.

Swart, H., Breytenbach, J.C., Hadgraft, J., du Plessis, J., 2005. Synthesis and transdermal penetration of NSAID glycoside esters. Int. J. Pharm. 301, 71–79.

Teichmann, A., Heuschkel, S., Jacobi, U., Presse, G., Neubert, R.H.H., Sterry, W., Lademann, J., 2007. Comparison of stratum corneum penetration and localization of a lipophilic model drug applied in an o/w microemulsion and an amphiphilic cream. Eur. J. Pharm. Biopharm. 66, 159–164.

Touitou, E., Fabin, B., 1988. Altered skin permeation of a highly lipophilic molecule: tetrahydrocannabinol. Int. J. Pharm. 43, 17–22.

Wagner, H., Zghoul, N., Lehr, C.M., Schäfer, U.F., 2002. Human skin and skin equivalents to study dermal penetration and permeation. In: Lehr, C.M. (Ed.), Cell Culture Models of Biological Barriers. Taylor and Francis, London, pp. 289–309.

Westesen, K., Bunjes, H., 1995. Do nanoparticles prepared from lipids solid at room temperature always possess a solid lipid matrix? Int. J. Pharm. 115, 129–131.

Wissing, S.A., Müller, R.H., 2002. The development of an improved carrier system for sunscreen formulations based on crystalline lipid nanoparticles. Int. J. Pharm. 242, 373–375.

Young, A.R., 2006. Acute effects of UVR on human eyes and skin. Prog. Biophys. Mol. Biol. 92, 80–85.